Synthesis, photophysical properties and *in vitro* photodynamic activity of axially substituted subphthalocyanines†

Hu Xu,[a] Xiong-Jie Jiang,[a] Elaine Y. M. Chan,[b] Wing-Ping Fong[b] and Dennis K. P. Ng*[a]

Received 20th August 2007, Accepted 15th October 2007
First published as an Advance Article on the web 30th October 2007
DOI: 10.1039/b712788j

A new series of subphthalocyanines substituted axially with an oligoethylene glycol chain [SPcB$(OCH_2CH_2)_nOH$, $n = 3$ (**2**) or 4 (**3**)] or a *p*-phenoxy oligoethylene glycol methyl ether chain [SPcB$OC_6H_4(OCH_2CH_2)_nOCH_3$, $n = 2$ (**4**) or 3 (**5**)] have been synthesised by substitution reactions of boron subphthalocyanine chloride SPcBCl (**1**) with the corresponding oligoethylene glycols, and characterised with various spectroscopic methods and elemental analysis. The molecular structure of one of these compounds (subphthalocyanine **4**) has also been determined. As revealed by absorption spectroscopy, these compounds are essentially non-aggregated in DMF. The low aggregation tendency of these compounds results in a strong fluorescence emission and high efficiency to generate singlet oxygen. All these subphthalocyanines, being formulated with Cremophor EL, function as efficient photosensitisers and exhibit a high photocytotoxicity against HepG2 human hepatocarcinoma and HT29 human colon adenocarcinoma cells. The phenoxy analogues **4** and **5** show a relatively high photostability and are particularly potent towards these cell lines, with IC_{50} values down to 0.02 μM.

Introduction

Photodynamic therapy (PDT) employs non-toxic photosensitisers and harmless visible light in combination with tissue oxygen to produce cytotoxic reactive oxygen species that destroy malignant cells and tissues by multifactorial mechanisms.[1] Much research effort has been put in the advancement of photosensitisers, which play a crucial role controlling the overall efficacy of PDT. Various tetrapyrrole derivatives such as porphyrins, chlorins and phthalocyanines have been studied extensively for this application.[2] Subphthalocyanines are regarded as the lower homologues of phthalocyanines with three diiminoisoindoline units N-fused around a boron centre.[3] Owing to the cone-shaped structure, these compounds show a much lower aggregation tendency and higher solubility than phthalocyanines. This feature, together with their delocalised 14-π-electron cores, lead to strong absorption and fluorescence emission in the orange–yellow visible region (*ca.* 560–600 nm). Preliminary photophysical studies have also found that these macrocycles can exhibit high triplet and singlet oxygen quantum yields,[4] making them potentially useful as photosensitisers for various photosensitising applications.

The early impetus for research into subphthalocyanines stemmed from their use in ring expansion reactions to prepare unsymmetrical A_3B-type phthalocyanines.[5] Recently, the focus has shifted to their technological applications, for example, as octupolar non-linear optical materials,[6] photovoltaic devices[7] and photosynthetic models for the study of photoinduced electron and energy transfer processes.[8] Recently, the use of these compounds as colorimetric and fluorometric molecular probes for cyanide and fluoride anions has also been reported.[9] To our knowledge, reports on the bio-medical applications of this class of functional dyes remain extremely rare.[10] We report herein the synthesis and characterisation of a new series of axially substituted subphthalocyanines and the first use of these compounds as efficient photosensitisers in PDT.

Results and discussion

The axially substituted subphthalocyanines **2–5** were prepared by typical substitution reactions of the commercially available boron subphthalocyanine chloride (**1**) with the corresponding alcohols in the presence of triethylamine in toluene (Scheme 1). These oligoethylene glycols were employed to increase the solubility and biocompatibility of the resulting subphthalocyanines. As a

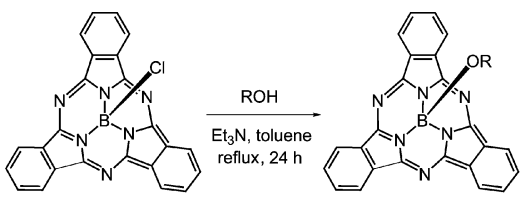

1

2 R = -$(CH_2CH_2O)_3H$ (5%)
3 R = -$(CH_2CH_2O)_4H$ (7%)
4 R = -$C_6H_4(OCH_2CH_2)_2OCH_3$ (30%)
5 R = -$C_6H_4(OCH_2CH_2)_3OCH_3$ (37%)

Scheme 1

[a]*Department of Chemistry and Centre of Novel Functional Molecules, The Chinese University of Hong Kong, Shatin, N.T., Hong Kong, China. E-mail: dkpn@cuhk.edu.hk; Fax: +852 2603 5057; Tel: +852 2609 6375*
[b]*Department of Biochemistry and Centre of Novel Functional Molecules, The Chinese University of Hong Kong, Shatin, N.T., Hong Kong, China*

† Electronic supplementary information (ESI) available: UV-Vis and fluorescence spectra of **2–5** in the DMEM and RPMI media; changes in the Q-band absorbance of **2–5** in the RPMI medium with time, both in the absence and presence of light; changes in absorption spectra of **2–5** in the presence of RNO and imidazole in the RPMI medium upon irradiation with time; ^1H and $^{13}C\{^1H\}$ NMR spectra of **2–5** in $CDCl_3$; crystal structure data for **4**. See DOI: 10.1039/b712788j

result, these compounds possessed a high solubility in many organic solvents and could be purified readily by silica-gel column chromatography followed by size exclusion chromatography with Bio-Beads S-X1 beads. The yields of the phenoxy analogues **4** and **5** (30–37%) were substantially higher than those of the alkoxy counterparts **2** and **3** (5–7%), which is in accord with the results for previously described alkoxy (OMe, OEt, O^{t}Bu and O^{i}Pr) and aryloxy subphthalocyanines.[3b,11]

Compounds **2–5** were fully characterised by various spectroscopic methods and elemental analysis. The ^{1}H NMR spectra of these compounds in $CDCl_3$ showed two typical AA′BB′ downfield multiplets (at δ 7.8–8.9) for the subphthalocyanine ring protons, and upfield-shifted signals for the axial substituents due to the shielding by the subphthalocyanine ring current. The molecular structure of compound **4** (Fig. 1) was also determined by X-ray diffraction analysis. Single crystals of this compound were grown by layering hexane onto a chloroform solution. The compound co-crystallises with one equiv. of solvated chloroform in the triclinic system with a $P\bar{1}$ space group. As shown in Fig. 1, the boron centre is tetra-coordinated, forming a cone-shaped structure. The B–O bond distance [1.440(4) Å] and the average B–N bond distance [1.496(5) Å] are comparable with those in the ethoxy analogue SPcBOEt [1.418(5) and 1.512(5) Å, respectively].[12]

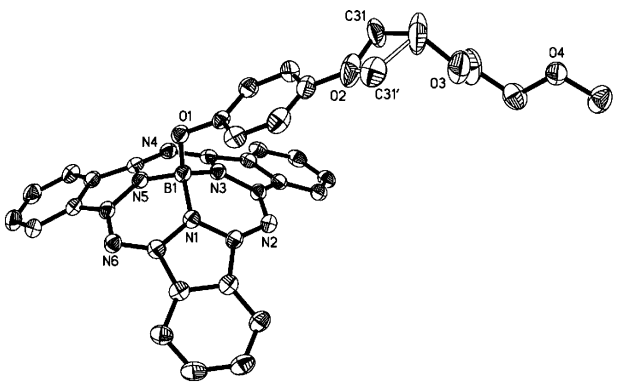

Fig. 1 Molecular structure of **4** showing the 30% probability thermal ellipsoids for all non-hydrogen atoms. The carbon atoms C31 and C31′ occupy a site with half occupancy.

The absorption spectra of compounds **2–5** in DMF are very similar, showing the B band at 301–302 nm, the Q band at 561–562 nm, together with a vibronic shoulder at 504–505 nm. The data are compiled in Table 1. The very similar spectra of these compounds indicate that the macrocyclic π system is not perturbed by the axial ligand. By plotting the Q-band absorbance *vs.* the concentration, a linear relationship was found for all these compounds, showing that they are essentially non-aggregated under these conditions. Due to the low aggregation tendency, these compounds were highly fluorescent. Upon excitation at 510 nm, these compounds emitted at 570–571 nm with a fluorescence quantum yield (Φ_f) of 0.56–0.58 (for **2** and **3**) or 0.20 (for **4** and **5**) relative to rhodamine B in ethanol ($\Phi_f = 0.49$) (Table 1).[13] The lower fluorescence quantum yields of the latter two compounds can be attributed to the presence of the phenoxy moiety, which partially quenches the fluorescence of the subphthalocyanine core by an intramolecular photo-induced electron transfer (PET) process.[14] Fig. 2 gives the absorption and fluorescence spectra of **4** in DMF, which are typical of the other subphthalocyanines.

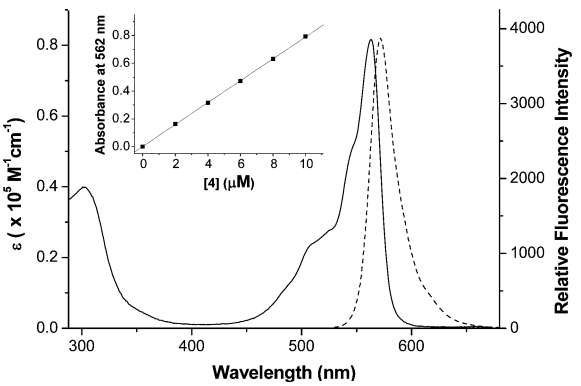

Fig. 2 Absorption (—) and fluorescence (---) spectra of **4** in DMF (2.0 μM). The inset plots the Q-band absorbance (at 562 nm) *vs.* the concentration of **4**, showing that the Lambert–Beer Law is followed.

To evaluate the photosensitising efficiency of these compounds, their singlet oxygen quantum yields (Φ_Δ) were also determined in ethanol by a steady-state method using 1,3-diphenylisobenzofuran (DPBF) as the scavenger. The concentration of the quencher was monitored spectroscopically at 410 nm with time, from which the values of Φ_Δ could be determined by the method described previously (Table 1).[15] As shown in Fig. 3, which compares the rates of decay of DPBF using **2–5** as the photosensitisers, all these subphthalocyanines can generate singlet oxygen. The alkoxy analogues **2** and **3** [$\Phi_\Delta = 0.64$–0.67 relative to rose bengal ($\Phi_\Delta = 0.68$)[16]] are much more effective than the phenoxy counterparts **4** and **5** ($\Phi_\Delta = 0.14$–0.15) in the generation of singlet oxygen in ethanol. This can be attributed to the absence of PET arising from the phenoxy moiety in **4** and **5**, thereby facilitating the intersystem crossing and photosensitisation processes.

The photodynamic activity of compounds **2–5** in Cremophor EL emulsions was investigated against two different cell lines, namely HepG2 human hepatocarcinoma and HT29 human colon adenocarcinoma cells. Due to the fact that the Q band of subphthalocyanines appears at a relatively short-wavelength position

Table 1 Electronic absorption and photophysical data for **2–5**

Compound	λ_{max}/nm (log ε)[a]	λ_{em}/nm [a,b]	Φ_f [a,c]	Φ_Δ [d,e]
2	301 (4.60), 504 (4.32), 561 (4.88)	570	0.58	0.67
3	301 (4.47), 505 (4.16), 561 (4.72)	570	0.56	0.64
4	302 (4.58), 505 (4.34), 562 (4.90)	571	0.20	0.15
5	302 (4.54), 505 (4.27), 562 (4.83)	571	0.20	0.14

[a] In DMF. [b] Excited at 510 nm. [c] Using rhodamine B in ethanol as the reference ($\Phi_f = 0.49$). [d] In ethanol. [e] Using rose bengal as the reference ($\Phi_\Delta = 0.68$).

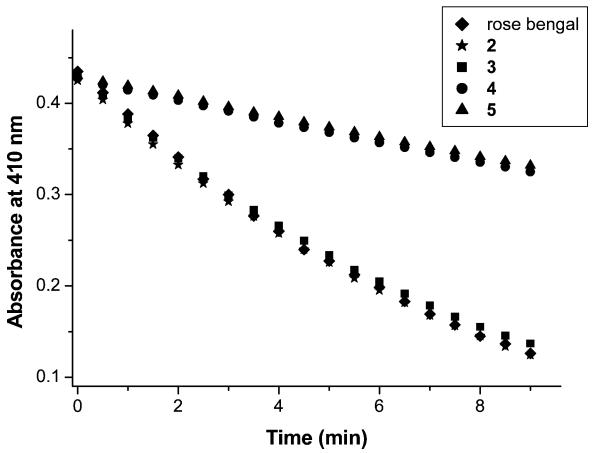

Fig. 3 Comparison of the rates of decay of DPBF in ethanol as monitored spectroscopically at 410 nm, using subphthalocyanines **2–5** as the photosensitisers and rose bengal as the reference.

(*ca.* 560 nm), a colour glass filter cut-on of 515 nm was used. Fig. 4 shows the dose-dependent survival curves for **2–5** on HepG2 and HT29. It can be seen that while these compounds are essentially

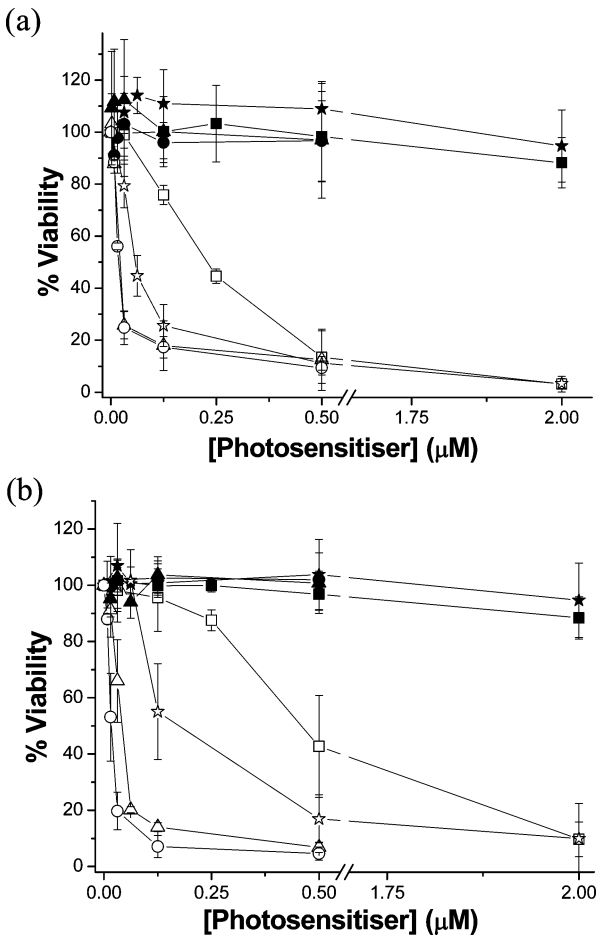

Fig. 4 Effects of **2** (stars), **3** (squares), **4** (circles) and **5** (triangles) on (a) HepG2 and (b) HT29 in the absence (closed symbols) and presence (open symbols) of light (λ > 515 nm, 49 mW cm^{-2}, 59 J cm^{-2}). Data are expressed as mean values ± standard error of the mean of three independent experiments, each performed in quadruplicate.

Table 2 Comparison of the IC_{50} values[a] of **2–5** against HepG2 and HT29

Compound	IC_{50}/μM	
	For HepG2	For HT29
2	0.06	0.17
3	0.23	0.46
4	0.02	0.02
5	0.02	0.04

[a] Defined as the dye concentration required to kill 50% of the cells.

non-cytotoxic in the absence of light (up to 2.0 μM), they exhibit a very high photocytotoxicity. The corresponding IC_{50} values, defined as the dye concentration required to kill 50% of the cells, are summarised in Table 2. Interestingly, although the phenoxy analogues **4** and **5** have a lower singlet oxygen quantum yield than the alkoxy counterparts **2** and **3** in ethanol (Table 1), they show a significantly higher photocytotoxicity, and the IC_{50} values are as low as 0.02 μM. For these two compounds, about 0.5 μM of the dye was sufficient to kill 90% of the cells, while for **2** and **3**, up to 2.0 μM of the dye was required.

The cellular uptake of these compounds was also examined by fluorescence microscopy. After incubation with these compounds (formulated with Cremophor EL) for 2 h and upon excitation at 490 nm (monitored at 500–575 nm), the HT29 cells showed a rather strong intracellular fluorescence as granular spots throughout the cytoplasm (Fig. 5). This observation indicated that there was substantial uptake of the dyes.

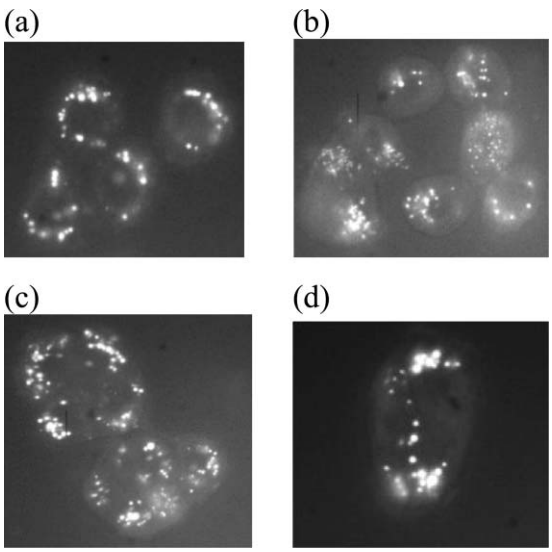

Fig. 5 Fluorescence images of HT29 cells incubated with (a) **2**, (b) **3**, (c) **4** and (d) **5** in Cremophor EL (8.0 μM) for 2 h (excited at 490 nm and monitored at 500–575 nm).

To account for the discrepancy in photocytotoxicity, we examined the stability of these compounds in the culture media by monitoring the decay of the Q band along with time. Initially, the UV-Vis spectra of **2–5** in these media resembled the corresponding spectra recorded in DMF, and all the compounds also showed a relatively strong fluorescence emission (Fig. S1†). These results suggested that these compounds are also essentially non-aggregated in the biological media. Fig. 6 shows the changes in

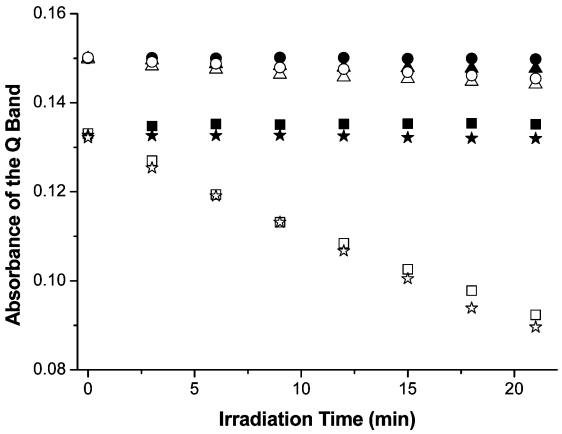

Fig. 6 Changes in the Q-band absorbance of **2** (stars), **3** (squares), **4** (circles) and **5** (triangles) in the DMEM medium (all at 2.0 μM) with time, both in the absence (closed symbols) and presence (open symbols) of light ($\lambda > 515$ nm, 9 mW cm^{-2}). The data were taken at 3 min intervals.

the Q-band absorbance of **2–5** in the DMEM medium (for HT29 cells) with time, both in the dark and under irradiation with yellow light ($\lambda > 515$ nm). It can be seen that, in the absence of light, the absorbance remains essentially unchanged for all the compounds, showing that they are stable in the medium in the dark. However, the alkoxy analogues **2** and **3** are unstable upon irradiation as shown by the rapid decrease in the Q-band absorbance. The values drop by 31–32% in 21 min, while those for the phenoxy analogues **4** and **5** decrease by only 3–4%. Similar results were observed in the RPMI medium 1640 (for HepG2 cells), in which the Q-band absorbance decreases by 23% for **2** and **3**, and 3–5% for **4** and **5** upon irradiation for 21 min (Fig. S2†). These observations clearly indicate that the latter two subphthalocyanines have a much higher photostability in the culture media.

The efficiency of these subphthalocyanines to generate singlet oxygen in the DMEM medium was also compared by the method reported by Kraljić and El Mohsni.[17] In this method, imidazole was used to capture singlet oxygen to form a transannular peroxide intermediate which can induce the bleaching of 4-nitrosodimethylaniline (RNO) as followed spectroscopically at 440 nm. While all the compounds induced a comparable decrease in the absorbance at 440 nm (15–19% after 21 min), the Q band of the alkoxy subphthalocyanines **2** and **3** diminished at a much faster rate than the phenoxy analogues **4** and **5** (57–59% *vs.* 9–11% after 21 min) (Fig. S3†). The results suggested that the higher singlet oxygen generation efficiency for **2** and **3** is counteracted by their lower photostability, leading to a comparable efficiency with **4** and **5**.

Conclusions

In summary, a new series of axially substituted subphthalocyanines **2–5** have been synthesised and characterised. These compounds exhibit a high photocytotoxicity against HepG2 and HT29 cells, with IC_{50} values down to 0.02 μM. The phenoxy subphthalocyanines **4** and **5** are more potent than the alkoxy counterparts **2** and **3**, which can be partly explained by their higher photostability. Further investigation to enhance the photodynamic activity and photostability of this new class of photosensitisers is underway.

Experimental

Experimental details regarding the purification of solvents, instrumentation, and *in vitro* studies are described elsewhere.[18] Triethylene glycol and tetraethylene glycol (Merck) were dried by azeotropic distillation with toluene prior to use.

4-(3,6-Dioxaheptoxy)phenol[19]

A mixture of hydroquinone (4.8 g, 43.6 mmol), 3,6-dioxaheptyl-4-toluenesulfonate (6.0 g, 21.9 mmol)[20] and potassium carbonate (9.0 g, 65.1 mmol) in acetonitrile (200 mL) was heated at reflux overnight. After cooling, the suspension was filtered and the filtrate was concentrated under reduced pressure. The residue was then chromatographed on a silica-gel column using $CHCl_3$–MeOH [from 100 : 1 to 40 : 1 (v/v) gradually] as eluent. The product was obtained as a pale yellow oil (2.2 g, 47%). ^{1}H NMR (300 MHz, $CDCl_3$): δ 6.72–6.79 (m, 4 H, Ar*H*), 5.04 (s, 1 H, ArO*H*), 4.05 (vt, $J = 4.9$ Hz, 2 H, ArOCH_2), 3.82 (vt, $J = 4.9$ Hz, 2 H, ArOCH$_2$CH_2), 3.70–3.73 (m, 2 H, CH_2), 3.57–3.60 (m, 2 H, CH_2), 3.40 (s, 3 H, CH_3); HRMS (ESI) calcd for $C_{11}H_{16}NaO_4$ [M + Na]$^+$ 235.0941, found 235.0943.

4-(3,6,9-Trioxadecoxy)phenol[19]

According to the above procedure, hydroquinone (10.0 g, 90.8 mmol) was treated with 3,6,9-trioxadecyl-4-toluenesulfonate (14.4 g, 45.2 mmol)[20] and potassium carbonate (18.7 g, 0.14 mol) in acetonitrile (200 mL) to give the product as a pale yellow oil (7.0 g, 60%). ^{1}H NMR (300 MHz, $CDCl_3$): δ 6.72–6.79 (m, 4 H, Ar*H*), 5.03 (s, 1 H, ArO*H*), 4.04 (vt, $J = 5.1$ Hz, 2 H, ArOCH_2), 3.82 (vt, $J = 5.1$ Hz, 2 H, ArOCH$_2$CH_2), 3.65–3.74 (m, 6 H, CH_2), 3.56–3.58 (m, 2 H, CH_2), 3.38 (s, 3 H, CH_3); HRMS (ESI) calcd for $C_{13}H_{20}NaO_5$ [M + Na]$^+$ 279.1203, found 279.1210.

General procedure for the preparation of 2–5

A mixture of boron subphthalocyanine chloride (**1**) (150 mg, 0.35 mmol), triethylamine (0.17 mL, 1.22 mmol) and the corresponding oligoethylene glycol (6 equiv. with respect to **1**) in toluene (10 mL) was heated at reflux for 24 h. After cooling, the volatiles were removed under reduced pressure, and the residue was loaded onto a silica-gel column and eluted with $CHCl_3$–MeOH (30 : 1, v/v). The crude product obtained was further purified by size exclusion chromatography with Bio-Beads S-X1 beads using THF as eluent. The final product was isolated as a violet solid.

Subphthalocyanine 2. Yield 5%; ^{1}H NMR (300 MHz, $CDCl_3$): δ 8.83–8.86 (m, 6 H, SPc-H_α), 7.86–7.89 (m, 6 H, SPc-H_β), 3.70 (t, $J = 4.5$ Hz, 2 H, CH_2OH), 3.46 (t, $J = 4.5$ Hz, 2 H, CH_2CH$_2$OH), 3.30 (t, $J = 4.5$ Hz, 2 H, CH_2), 3.06 (t, $J = 4.5$ Hz, 2 H, CH_2), 2.57 (t, $J = 4.8$ Hz, 2 H, BOCH$_2$CH_2), 1.66 (t, $J = 4.8$ Hz, 2 H, BOCH_2); ^{13}C{^{1}H} NMR (75.4 MHz, $CDCl_3$): δ 151.4, 130.9, 129.7, 122.1, 72.6, 70.9, 70.1, 65.9, 61.9, 58.7; HRMS (ESI) calcd for $C_{30}H_{25}BN_6NaO_4$ [M + Na]$^+$ 567.1923, found 567.1917. Anal. Calcd for $C_{30}H_{25}BN_6O_4$: C, 66.19; H, 4.63; N, 15.44. Found: C, 66.65; H, 4.87; N, 15.66.

Subphthalocyanine 3. Yield 7%; ^{1}H NMR (300 MHz, $CDCl_3$): δ 8.83–8.89 (m, 6 H, SPc-H_α), 7.87–7.92 (m, 6 H, SPc-H_β), 3.70–3.76 (m, 2 H, CH_2OH), 3.53–3.58 (m, 4 H, CH_2), 3.38–3.42 (m, 2 H, CH_2), 3.24–3.27 (m, 2 H, CH_2), 3.04–3.08 (m, 2 H, CH_2), 2.56 (t, $J = 5.1$ Hz, 2 H, BOCH$_2$CH_2), 1.64 (t, $J = 5.1$ Hz, 2 H, BOCH_2); ^{13}C{^{1}H} NMR (75.4 MHz, $CDCl_3$): δ 151.4, 130.9, 129.7, 122.1, 72.6, 70.8, 70.4, 70.3, 70.1, 70.0, 61.7, 58.6; HRMS (ESI) calcd for $C_{32}H_{29}BN_6NaO_5$ $[M + Na]^+$ 611.2185, found 611.2190. Anal. Calcd for $C_{33}H_{33}BN_6O_6$ (**3**·MeOH): C, 63.88; H, 5.36; N, 13.54. Found: C, 64.01; H, 4.95; N, 13.66.

Subphthalocyanine 4. Yield 30%; ^{1}H NMR (300 MHz, $CDCl_3$): δ 8.83–8.86 (m, 6 H, SPc-H_α), 7.89–7.92 (m, 6 H, SPc-H_β), 6.30 (d, $J = 9.0$ Hz, 2 H, C$_6H_4$), 5.34 (d, $J = 9.0$ Hz, 2 H, C$_6H_4$), 3.86–3.89 (m, 2 H, CH_2), 3.69–3.71 (m, 2 H, CH_2), 3.61–3.64 (m, 2 H, CH_2), 3.49–3.53 (m, 2 H, CH_2), 3.36 (s, 3 H, CH_3); ^{13}C{^{1}H} NMR (75.4 MHz, $CDCl_3$): δ 153.4, 151.2, 146.1, 130.9, 129.8, 122.2, 119.9, 114.8, 71.9, 70.6, 69.8, 67.5, 59.0; HRMS (ESI) calcd for $C_{35}H_{27}BN_6NaO_4$ 629.2079, found 629.2078. Anal. Calcd for $C_{35}H_{27}BN_6O_4$: C, 69.32; H, 4.49; N, 13.86. Found: C, 69.60; H, 4.62; N, 13.83.

Subphthalocyanine 5. Yield 37%; ^{1}H NMR (300 MHz, $CDCl_3$): δ 8.81–8.85 (m, 6 H, SPc-H_α), 7.86–7.91 (m, 6 H, SPc-H_β), 6.30 (d, $J = 9.0$ Hz, 2 H, C$_6H_4$), 5.32 (d, $J = 9.0$ Hz, 2 H, C$_6H_4$), 3.84–3.87 (m, 2 H, CH_2), 3.70–3.73 (m, 2 H, CH_2), 3.60–3.67 (m, 6 H, CH_2), 3.49–3.53 (m, 2 H, CH_2), 3.35 (s, 3 H, CH_3); ^{13}C{^{1}H} NMR (75.4 MHz, $CDCl_3$): δ 153.3, 151.2, 146.0, 130.9, 129.7, 122.2, 119.9, 114.8, 71.9, 70.7, 70.6, 70.5, 69.7, 67.5, 59.0; HRMS (ESI) calcd for $C_{37}H_{31}BN_6NaO_5$ 673.2341, found: 673.2341. Anal. Calcd for $C_{37}H_{31}BN_6O_5$: C, 68.32; H, 4.80; N, 12.92. Found: C, 67.93; H, 5.17; N, 12.56.

X-Ray crystallographic analysis of 4·CHCl$_3$

Crystal data and details of data collection and structure refinement are given in Table 3. Data were collected on a Bruker SMART CCD diffractometer with an MoKα sealed tube ($\lambda = 0.71073$ Å) at 293 K, using a ω scan mode with an increment of 0.3°. Preliminary unit cell parameters were obtained from 45 frames. Final unit cell parameters were obtained by global refinements of reflections obtained from integration of all the frame data. The collected frames were integrated using the preliminary cell-orientation matrix. SMART software was used for collecting frames of data, indexing reflections and determination of lattice constants; SAINT-PLUS for integration of intensity of reflections and scaling;[21] SADABS for absorption correction;[22] and SHELXL for space group and structure determination, refinements, graphics and structure reporting.[23] CCDC reference number 658016. For crystallographic data in CIF or other electronic format see DOI: 10.1039/b712788j.

Acknowledgements

This work was supported by a grant from the Research Grants Council of the Hong Kong Special Administrative Region, China (Project No. 402607), and a strategic investments scheme administered by The Chinese University of Hong Kong.

Table 3 Crystallographic data for **4**·CHCl$_3$

Formula	$C_{36}H_{28}BCl_3N_6O_4$
M_r	725.80
Crystal size/mm^3	0.50 × 0.40 × 0.30
Crystal system	Triclinic
Space group	$P\bar{1}$
a/Å	8.8675(12)
b/Å	12.5714(17)
c/Å	16.873(2)
α/°	77.372(3)
β/°	85.404(3)
γ/°	69.451(2)
V/Å^3	1718.6(4)
Z	2
$F(000)$	748
ρ_{calcd}/Mg m^{-3}	1.403
μ/mm^{-1}	0.316
θ range/°	1.77–25.00
Reflections collected	9303
Independent reflections	5993 ($R_{int} = 0.0206$)
Parameters	461
$R1$ [$I > 2\sigma(I)$]	0.0680
w$R2$ [$I > 2\sigma(I)$]	0.1870
Goodness of fit	1.020

References and notes

1 (*a*) D. E. J. G. J. Dolmans, D. Fukumura and R. K. Jain, *Nat. Rev. Cancer*, 2003, **3**, 380; (*b*) S. B. Brown, E. A. Brown and I. Walker, *Lancet Oncol.*, 2004, **5**, 497; (*c*) A. P. Castano, P. Mroz and M. R. Hamblin, *Nat. Rev. Cancer*, 2006, **6**, 535.
2 (*a*) H. Ali and J. E. van Lier, *Chem. Rev.*, 1999, **99**, 2379; (*b*) M. R. Detty, S. L. Gibson and S. J. Wagner, *J. Med. Chem.*, 2004, **47**, 3897; (*c*) E. S. Nyman and P. H. Hynninen, *J. Photochem. Photobiol. B*, 2004, **73**, 1.
3 (*a*) M. Geyer, F. Plenzig, J. Rauschnabel, M. Hanack, B. del Rey, A. Sastre and T. Torres, *Synthesis*, 1996, 1139; (*b*) C. G. Claessens, D. González-Rodríguez and T. Torres, *Chem. Rev.*, 2002, **102**, 835.
4 S. Nonell, N. Rubio, B. del Rey and T. Torres, *J. Chem. Soc., Perkin Trans. 2*, 2000, 1091.
5 See for example: (*a*) N. Kobayashi, R. Kondo, S.-i. Nakajima and T. Osa, *J. Am. Chem. Soc.*, 1990, **112**, 9640; (*b*) A. Weitemeyer, H. Kliesch and D. Wöhrle, *J. Org. Chem.*, 1995, **60**, 4900; (*c*) A. Sastre, B. del Rey and T. Torres, *J. Org. Chem.*, 1996, **61**, 8591.
6 See for example: (*a*) A. Sastre, T. Torres, M. A. Díaz-García, F. Agulló-López, C. Dhenaut, S. Brasselet, I. Ledoux and J. Zyss, *J. Am. Chem. Soc.*, 1996, **118**, 2746; (*b*) B. del Rey, U. Keller, T. Torres, G. Rojo, F. Agulló-López, S. Nonell, C. Martí, S. Brasselet, I. Ledoux and J. Zyss, *J. Am. Chem. Soc.*, 1998, **120**, 12808; (*c*) D. Dini, S. Vagin, M. Hanack, V. Amendola and M. Meneghetti, *Chem. Commun.*, 2005, 3796.
7 K. L. Mutolo, E. I. Mayo, B. P. Rand, S. R. Forrest and M. E. Thompson, *J. Am. Chem. Soc.*, 2006, **128**, 8108.
8 (*a*) D. González-Rodríguez, T. Torres, D. M. Guldi, J. Rivera and L. Echegoyen, *Org. Lett.*, 2002, **4**, 335; (*b*) D. González-Rodríguez, T. Torres, D. M. Guldi, J. Rivera, M. Á. Herranz and L. Echegoyen, *J. Am. Chem. Soc.*, 2004, **126**, 6301; (*c*) R. S. Iglesias, C. G. Claessens, T. Torres, G. M. Aminur Rahman and D. M. Guldi, *Chem. Commun.*, 2005, 2113; (*d*) D. González-Rodríguez, C. G. Claessens, T. Torres, S. Liu, L. Echegoyen, N. Vila and S. Nonell, *Chem. Eur. J.*, 2005, **11**, 3881; (*e*) D. González-Rodríguez, T. Torres, M. M. Olmstead, J. Rivera, M. Á. Herranz, L. Echegoyen, C. A. Castellanos and D. M. Guldi, *J. Am. Chem. Soc.*, 2006, **128**, 10680.
9 (*a*) S. Xu, K. Chen and H. Tian, *J. Mater. Chem.*, 2005, **15**, 2676; (*b*) J. V. Ros-Lis, R. Martínez-Máñez and J. Soto, *Chem. Commun.*, 2005, 5260; (*c*) E. Palomares, M. V. Martínez-Díaz, T. Torres and E. Coronado, *Adv. Funct. Mater.*, 2006, **16**, 1166.
10 K. Adachi and H. Watarai, *Anal. Chem.*, 2006, **78**, 6840.
11 K. Adachi and H. Watarai, *Chem. Eur. J.*, 2006, **12**, 4249.
12 K. Kasuga, T. Idehara, M. Handa, Y. Ueda, T. Fujiwara and K. Isa, *Bull. Chem. Soc. Jpn.*, 1996, **69**, 2559.
13 K. G. Casey and E. L. Quitevis, *J. Phys. Chem.*, 1988, **92**, 6590.

14 The overall free energy change (ΔG°) for this PET process was estimated to be −0.68 eV by the Rehm–Weller equation: $\Delta G^\circ = e[E_{1/2}(D^{\bullet+}/D) - E_{1/2}(A/A^{\bullet-})] - \Delta E(0,0) - w_p$, where e is the charge on the electron, $E_{1/2}$ is the half-wave reduction potential for either the donor ($D^{\bullet+}/D$) or acceptor ($A/A^{\bullet-}$) couples in volts, $\Delta E(0,0)$ is the relevant singlet state energy, and w_p is a Coulombic interaction term between the oxidised donor and reduced acceptor (D. Rehm and A. Weller, *Isr. J. Chem.*, 1970, **8**, 259), showing that this is a thermodynamically favourable process. In the calculation, the reduction potentials of the model compounds 4-ethoxyphenol [$E_{1/2}(D^{\bullet+}/D) = 0.41$ V] (L. Meites, P. Zuman, W. J. Scott, B. H. Campbell and A. M. Kardos, *Electrochemical Data. Part 1: Organic, Organometallic, and Biochemical Substances, Volume A*, Wiley, New York, 1974, p. 347), and SPcBOMe [$E_{1/2}(A/A^{\bullet-}) = -1.10$ V][12] were taken. The singlet state energy was estimated to be 2.19 eV from the intersection position (567 nm) of the absorption and fluorescence spectra of **4**. In polar solvents, the w_p term is usually small (<0.1 eV) and was neglected in the calculation.
15 (*a*) W. Spiller, H. Kliesch, D. Wöhrle, S. Hackbarth, B. Röder and G. Schnurpfeil, *J. Porphyrins Phthalocyanines*, 1998, **2**, 145; (*b*) M. D. Maree, N. Kuznetsova and T. Nyokong, *J. Photochem. Photobiol. A*, 2001, **140**, 117.
16 R. W. Redmond and J. N. Gamlin, *Photochem. Photobiol.*, 1999, **70**, 391.
17 I. Kraljić and S. El Mohsni, *Photochem. Photobiol.*, 1978, **28**, 577.
18 P.-C. Lo, C. M. H. Chan, J.-Y. Liu, W.-P. Fong and D. K. P. Ng, *J. Med. Chem.*, 2007, **50**, 2100.
19 These compounds have been briefly described (see A. Siddiqui, C. McGuigan, C. Ballatore, S. Srinivasan, E. De Clercq and J. Balzarini, *Bioorg. Med. Chem. Lett.*, 2000, **10**, 381); but no characterisation data were given.
20 H. Brunner and N. Gruber, *Inorg. Chim. Acta*, 2004, **357**, 4423.
21 *SMART and SAINT for Windows NT Software Reference Manuals*, Version 5.0, Bruker Analytical X-ray Systems, Madison, WI, 1997.
22 G. M. Sheldrick, *SADABS – Software for Empirical Absorption Correction*, University of Göttingen, Germany, 1997.
23 *SHELXL Reference Manual*, Version 5.1, Bruker Analytical X-ray Systems, Madison, WI, 1997.

